ORIGINAL PAPER

Friction Reduction in Elastohydrodynamic Contacts by Thin-Layer Thermal Insulation

M. Björling · W. Habchi · S. Bair · R. Larsson ·
P. Marklund

Abstract Reducing friction is of utmost importance to improve efficiency and lifetime of many products used in our daily lives. Thin hard coatings like diamond-like carbon (DLC) have been shown to reduce friction in full-film-lubricated contacts. In this work, it is shown that contrarily to common belief, the friction reduction stems mainly from a thermal phenomenon and not only a chemical/surface interaction one. It is shown that a few micrometer-thin DLC coating can significantly influence the thermal behavior in a lubricated mechanical system. The presented simulations, validated by experiments, show that applying a thin DLC coating to metal surfaces creates an insulating effect that due to the increased liquid lubricant film temperature at the center of the contact, locally reduces lubricant viscosity and thus friction. The results of the investigation show that the addition of thin insulating layers could lead to substantial performance increases in many applications. On a component level, the contact friction coefficient in some common machine components like gears, rolling element bearings, and cam followers can potentially be reduced by more than 40 %. This will most likely open up the way to new families of coatings with a focus on thermal properties that may be both cheaper and more suitable in certain applications than DLC coatings.

List of symbols

β_K	Temperature coefficient of K_0 (K^{-1})
χ	Dimensionless heat capacity scaling parameter
η	Generalized (shear dependent) viscosity (Pa s)
γ	Shear rate (s^{-1})
κ	Dimensionless conductivity scaling parameter
Λ	Limiting stress pressure coefficient
λ_R	Relaxation time at T_R and ambient pressure (s)
μ	Limiting low-shear viscosity (Pa s)
μ_R	Low shear viscosity at T_R and ambient pressure (Pa s)
μ_∞	Viscosity extrapolated to infinite temperature (Pa s)
ρ	Lubricants density (kg)
τ	Shear stress (Pa)
τ_L	Limiting shear stress (Pa)
φ	Dimensionless viscosity scaling parameter
φ_∞	Viscosity scaling parameter for unbounded viscosity
A	Coefficient in the dimensionless conductivity scaling parameter
a_v	Thermal expansivity defined for volume linear with temperature (K^{-1})
B_F	Fragility parameter in the new viscosity equation
C_0	Parameter in the heat capacity function (J/m^3 K)
C_k	Parameter in the conductivity function (W/m K)
c_p	Specific heat capacity (J/kg K)
C_v	Lubricants volumetric heat capacity
F	Load (N)

M. Björling (✉) · R. Larsson · P. Marklund
Division of Machine Elements, Department of Engineering
Science and Mathematics, Luleå University of Technology,
97187 Luleå, Sweden
e-mail: marcus.bjorling@ltu.se

W. Habchi
Department of Industrial and Mechanical Engineering, Lebanese
American University, Byblos, Lebanon

S. Bair
Georgia Institute of Technology, Centre for High Pressure
Rheology, G.W. Woodruff School of Mechanical Engineering,
Atlanta, GA 30332-0405, USA

| G	Effective shear modulus (Pa)
g	Thermodynamic interaction parameter
k	Thermal conductivity (W/m K)
K_0'	Pressure rate of change of isothermal bulk modulus at $p = 0$
K_{00}	K_0 at zero absolute temperature (Pa)
K_0	Isothermal bulk modulus at $p = 0$ (Pa)
L	Contact load (N)
m	Parameter in the heat capacity function (J/m^3 K)
n	Power law exponent
p	Pressure (Pa)
q	Coefficient in the dimensionless conductivity scaling parameter
R	Ball radius (m)
s	Exponent in the conductivity scaling model
SRR	Slide to roll ratio
T	Temperature (K)
T_R	Reference temperature (K)
U_e	Mean entrainment speed (m/s)
u_i	Surface velocity (m/s)
V	Volume (m^3)
V_0	Volume at $p = 0$ (m^3)
V_R	Volume at reference state, T_R, $p = 0$ (m^3)

1 Introduction

Hydrodynamic lubrication (HL) has been studied for more than a century since its discovery by Beauchamp Tower [30]. Osborne Reynolds derived the governing equation of HL (which bears his name) from the Navier–Stokes equations [25]. Elastohydrodynamic lubrication (EHL) was discovered half a century later. Due to the nonconformal contacts found in systems working in EHL, the contact pressure is sufficient to cause elastic deformation of the contacting surfaces and many orders of magnitude increase of viscosity of the liquid film. Increased understanding in this field is crucial for improvements of machine components such as bearings, gears, and cam followers, as well as implants for the human knee and hip joints. To reduce friction in EHL contacts, researchers have been focusing on the development of new lubricants to reduce shear forces and surface finishing techniques to reduce asperity interactions between the surfaces. More recently, coatings have been investigated to increase wear resistance and reduce friction in case of solid contact. High hardness, high elastic modulus, low friction characteristics, high wear and corrosion resistance, chemical inertness, and thermal stability are factors that make diamond-like carbon (DLC) coatings the subject of much investigation. These factors make the coatings promising for use in, among others, machine components and cutting tools. Of interest in this study is, however, the low thermal conductivity (in the range of 1–3 W/mK) that has been measured for these thin coatings [4, 20, 26].

Reports of friction reduction with DLC-coated surfaces in full-film EHL have been published earlier [6, 10, 32]. This reduction has been attributed by several authors to boundary slip [10, 18, 19] as a consequence of non-fully wetted surfaces [8, 17, 23, 24, 27–29, 31, 34], where some of the work is based on atomically smooth surfaces. Slip at the boundary would lead to lower shear stresses and thus lower friction in the EHL contact. It has also been observed that for boundary slip to take place, three factors must be fulfilled. First of all, the surface has to be non- or partially wetted by the lubricant. Secondly, the pressure must be low, close to ambient where the lubricant would still be in its liquid form, opposed to the glass state at higher pressures. Finally, the surfaces must be very smooth, generally below 6 nm RMS [8, 27, 28, 35]. However, the present authors have presented an investigation in which friction reduction with DLC coatings was measured [6] in the EHL full-film regime even when the combined RMS roughness of the surfaces was in the range of 155–355 nm. Based on a simplified analytical estimation of the temperature increase in the lubricant film induced by DLC surface coating, the authors proposed that the friction reduction could be a result of thermal insulation due to the low thermal conductivity observed for some DLC coatings. The temperature increase in the lubricant film would reduce the viscosity and thereby reduce the coefficient of friction. It was also shown that coating only one of the specimens reduced the friction coefficient, albeit not as much as when both surfaces were coated. In this article, a more advanced and thoroughly validated [12, 13, 15] 3D numerical model was used to predict the effect of thin insulating layers on full-film EHL friction. A series of friction experiments have also been conducted in a ball-on-disk machine where an uncoated pair of specimens is compared to a pair of DLC-coated specimens to validate the numerical results.

2 Overall Methodology

The following sections cover the investigated cases, including running conditions and loads. It also contains information about the lubricant and its transport properties, as well as the numerical model and the underlying boundary conditions and assumptions. Finally, the experimental equipment, specimens, and coating are discussed together with the test procedure. A schematic of the experimental and numerical model setup can be seen in Fig. 1.
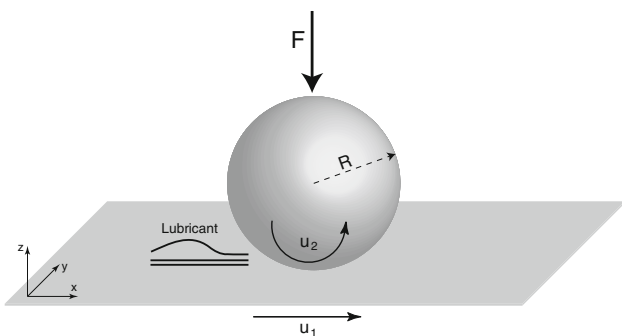
Fig. 1 Schematic of the experimental and numerical model of the studied system. F is the applied load, R is the radius of the ball and u_1, u_2 the surface velocities of the disk and ball. Slide-to-roll ratio is defined as $u_1 - u_2/(u_1 + u_2/2)$

2.1 Investigation Procedure

The numerical prediction and experimental measurements are performed using the same conditions reported in Table 1. SRR is defined as the velocity difference divided by the mean entrainment velocity, U_e. All tests are performed with positive sliding only, which in this case means that the ball is rotating faster than the disk.

Both numerical predictions and experiments were performed with the same lubricant, squalane, a commercially available low molecular weight branched alkane (2,6,10,15,19,23-hexamethyltetracosane). Oil without additives was chosen to minimize the effect of tribo-chemical reactions on the friction coefficient. At the test temperature of 40 °C, the ambient viscosity of squalane is 15 mPas and the pressure viscosity coefficient is 18 GPa^{-1} [1]. The following section gives a more in depth view of the lubricant parameters used in the numerical model.

2.2 Lubricant Transport Properties

The transport properties used for the numerical model in this study are obtained from several earlier studies on squalane. A brief overview of the models derived from these studies is given here. Further information about the measurements for the effect of pressure, temperature, and shear on viscosity is found in references: [1–3].

2.2.1 Equation of State

A temperature modified version of the Tait equation of state is used to model the temperature- and pressure-dependence of volume for squalane. The Tait equation is written for the volume relative to the volume at ambient pressure,

Table 1 Investigated conditions

Temperature	40 °C
Contact load	80 and 300 N
Maximum hertzian pressure	1.25 and 1.94 GPa
Entrainment speed, U_e	3.145 and 6.144 m/s
Slide-to-roll ratio, SRR	0.0002–1.05
Coating	None or Tribobond 43

$$\frac{V}{V_0} = 1 - \frac{1}{1 + K_0'} ln\left[1 + \frac{p}{K_0}(1 + K_0')\right] \tag{1}$$

with

$$K_0 = K_{00}\exp(-\beta_K T) \tag{2}$$

The volume at ambient pressure relative to the ambient pressure volume at the reference temperature, T_R, is assumed to vary with temperature as:

$$\frac{V_0}{V_R} = 1 + a_v(T - T_R) \tag{3}$$

where $K_0' = 11.74, a_v = 8.36 \times 10^{-4} K^{-1}, K_{00} = 8.658$ GPa and $\beta_K = 6.332 \times 10^{-3}\ K^{-1}$ were obtained from experimental measurements with a standard deviation of 0.05 % [1].

2.2.2 Viscosity

A thermodynamic scaling rule has been found to be accurate for many organic liquids is: $\mu = f(TV^g)$, where -3 g is related to the exponent of the repulsive intermolecular potential. A useful scaling parameter can therefore be written as:

$$\varphi = \left(\frac{T}{T_R}\right)\left(\frac{V}{V_R}\right)^g \tag{4}$$

An accurate scaling function can be obtained from a Vogel-like form:

$$\mu = \mu_\infty \exp\left(\frac{B_F \varphi_\infty}{\varphi - \varphi_\infty}\right) \tag{5}$$

where $g = 3.921$, $\varphi_\infty = 0.1743, B_F = 24.50$ and $\mu_\infty = 0.9506 \times 10^{-4}\ Pa\,s$ were obtained from experimental measurements with standard deviation of 14.9 % with respect to relative viscosity [1].

For the shear-dependence of viscosity, a t-T-p shifted Carreau equation is used:

$$\eta(\gamma, T, p) = \mu\left[1 + \left(\gamma \lambda_R \frac{\mu}{\mu_R}\frac{T_R}{T}\frac{V}{V_R}\right)^2\right]^{(n-1)/2} \tag{6}$$

where $\mu_R = 15.6$ mPa s, $\lambda_R = 2.26 \times 10^{-9}$ s, and $n = 0.463$ were obtained from Non-Equilibrium Molecular Dynamics and experimental measurements [3].

The limiting shear stress was shown to depend on pressure as:

$$\tau_L = \Lambda p \tag{7}$$

where $\Lambda = 0.075$ was found from EHL traction experiments and is assumed to be independent of temperature [2].

2.2.3 Thermal Properties

The thermal conductivity and volumetric heat capacity of squalane are expressed as:

$$k = C_k \kappa^{-s} \tag{8}$$

with

$$\kappa = \left(\frac{V}{V_R}\right)\left[1 + A\left(\frac{T}{T_R}\right)\left(\frac{V}{V_R}\right)^q\right] \tag{9}$$

where $q = 2$ and $A = -0.115$, and

$$C_v = \rho c_p = C_0 + m\chi \tag{10}$$

with

$$\chi = \left(\frac{T}{T_R}\right)\left(\frac{V}{V_R}\right)^{-3} \tag{11}$$

where $C_k = 0.074$ W/m K, $s = 4.5$, $C_0 = 0.94 \times 10^6$ J/m^3 K and $m = 0.62 \times 10^6$ J/m^3 K were obtained from experimental measurements. The thermal properties were measured by Ove Andersson at Umeå University.

2.3 Numerical Model

The numerical model employed in this work is based on the full-system finite element approach for thermal elastohydrodynamic lubricated (TEHL) contacts described in details in [12, 14, 15]. In this section, only the main features of this model are recalled along with the necessary amendments required for the inclusion of surface coatings. The model is based on a finite element fully coupled resolution of the EHL equations: Reynolds, linear elasticity, and load balance equations. The latter are solved simultaneously providing robust and fast-converging solutions. The generalized Reynolds equation [33] is used to account for the shear-dependence of the lubricant. Special formulations are introduced in order to stabilize the solution of Reynolds equation at high loads. The inclusion of coatings into the EHL model consists simply in adding a thin layer to the surface of the 3D solid body representing the contacting solids. This layer possesses different elastic material properties than those of the substrate. However, the simulation of a typical isothermal Newtonian EHL line contact with DLC coatings of different thickness shows that for coatings of 2–5-μm thickness (such as the ones considered in this work), the effect of the coating on dimensionless film thickness and pressure is negligible as suggested by Figs. 2 and 3. Therefore, for the sake of simplicity, in the EHL part of the model, the surfaces are assumed to be uncoated and the coatings are only considered in the thermal part. This leads to a significant reduction in the size of the discrete problem as the thin-layer coating requires a very large number of elements to discretize it. However, the influence of hard coatings on EHL
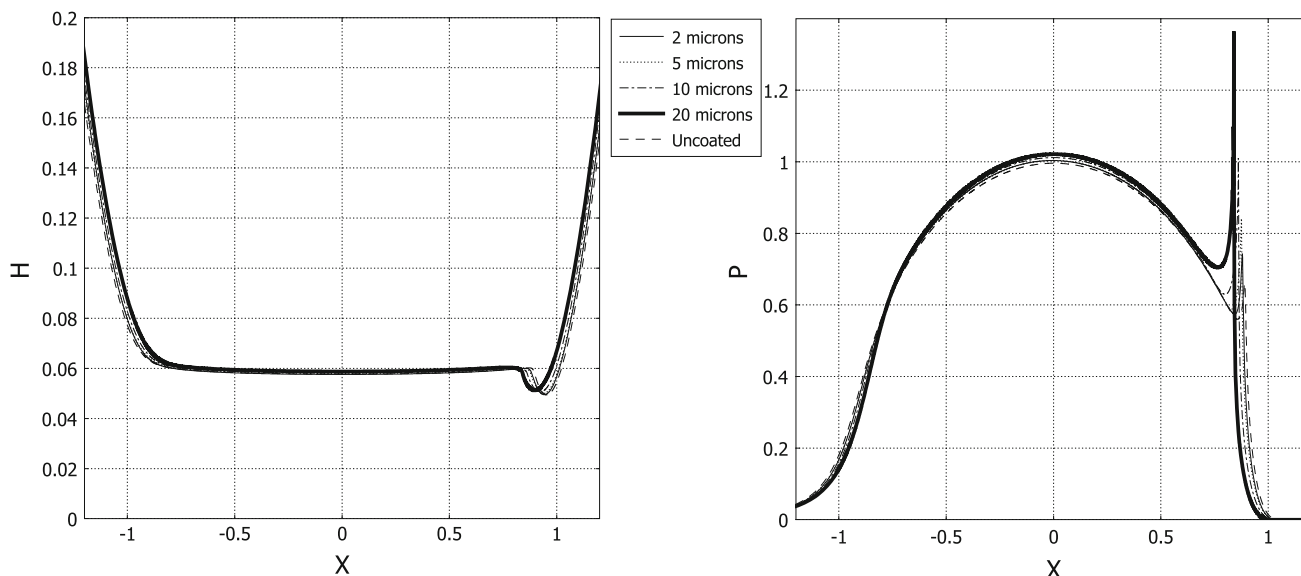
Fig. 2 Effect of DLC-coating thickness on the dimensionless film thickness (*left*) and pressure (*right*) distribution of a typical EHL line contact
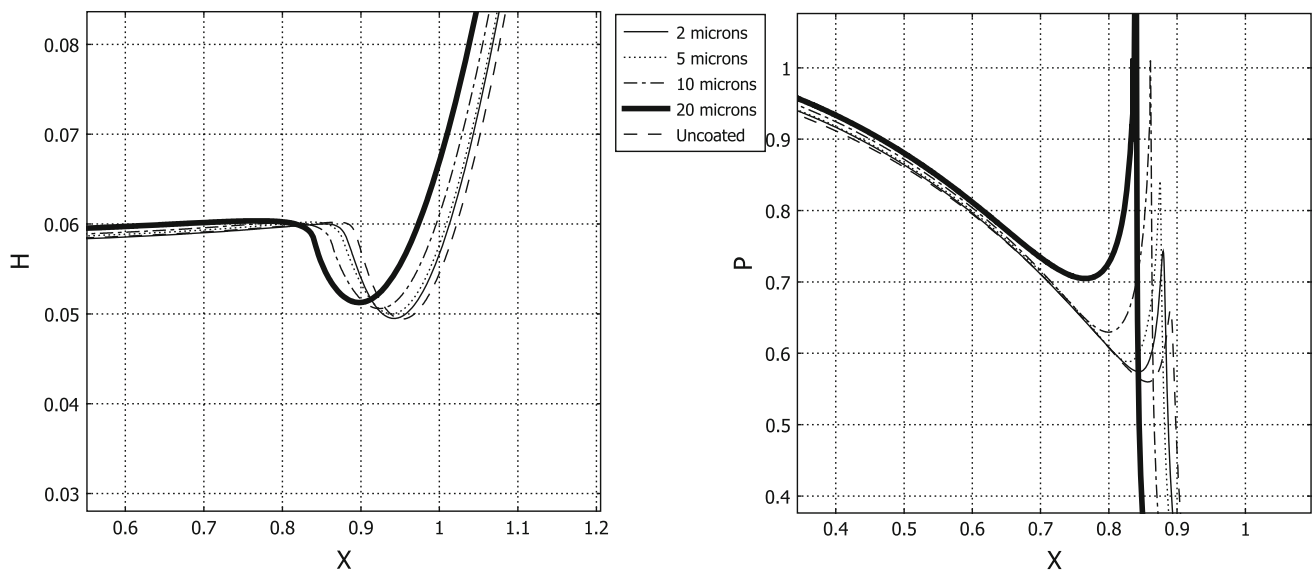
Fig. 3 Effect of DLC-coating thickness on the dimensionless film thickness (*left*) and pressure (*right*) distribution of a typical EHL *s* contact (Zoom on Fig. 2)

Table 2 Specimen material properties

Material	52100 (AISI)	Tribobond 43
Young's modulus (Pa)	210×10^9	–
Poisson's coefficient	0.3	–
Specific heat capacity (J/kg K)	475	1,000
Thermal conductivity (W/m K)	46.6	2.225
Density (kg/m^3)	7,850	2,500

film formation and pressure distribution has been studied in several publications [9, 21, 22]. It is shown (as also seen in Figs. 2 and 3) that a coating that is harder than the substrate reduces the contact width and increases the central pressure and the pressure spike. A coating that is softer than the substrate would have the opposite effect. Both effects increase with the thickness of the coating. The temperature distribution in the contact is obtained by solving the 3D energy equation in the lubricant film and solid bodies (substrates and coatings). The inclusion of the coatings consists in inserting a geometrical layer between the lubricant and each substrate and applying the thermal properties of DLC to it. Obviously, the continuity of heat flux needs to be imposed between the lubricant film and the coatings as well as between the coatings and the substrates. The model incorporates the variations of the lubricant's thermal properties with pressure and temperature throughout the contact. An iterative procedure is established between the respective solutions of the EHL and thermal problems as described in [12, 14]. Throughout the iterative procedure, every time the shear stress τ is evaluated (using viscosity data provided by a combination of the Carreau and Vogel-like models), it is either truncated to τ_L

if it exceeds τ_L or, otherwise, it is kept unchanged. The numerical model does not take asperity interactions into account and should therefore in this design only be seen as a full-film EHL model.

2.4 Ball-on-Disk Tribotester

The experiments were carried out with a Wedeven Associates Machine (WAM) 11, ball-on-disk test device. The lubricant is supplied at the center of the disk in an oil dispenser that distributes the lubricant across the disk surface. Lubricant is circulated in a closed loop from the oil bath, through a peristaltic pump to the oil dispenser at the center of the disk. The peristaltic pump is delivering approximately 180 ml/min. Three thermocouples are used in the test setup, one located in the oil bath, one in the outlet of the oil supply, and one trailing in the oil film close to the inlet region of the ball-on-disk contact. A more thorough description of the test rig and its features is presented in previous work [7].

2.4.1 Test Specimens

All specimens used in the tests (balls and disks) are made from AISI 52100 bearing steel. The balls are grade 20 with a 13/16 inch (20.637 mm) outer diameter and a hardness of about 60 HRC. The disks have a 4 inch (101.6 mm) outer diameter, a circumferential grind (before polish) and are through hardened to about 60 HRC. Additional material parameters also used in the numerical model are found in Table 2. The tests (and predictions) were performed with both uncoated 52100 (AISI) specimens and specimens

coated with Tribobond 43 (hydrogenated amorphous carbon (Cr+) a–C:H), a commercially available DLC coating applied through plasma-assisted chemical vapor deposition, measured to a thickness of 2.8 μm using calotest. The surface roughness, RMS, has been measured to about 25 nm for the balls and 35 nm for the disk, which gives a combined roughness of approximately 43 nm. The surface roughness measurements have been conducted in a Wyko NT1100 optical profilometer system from Veeco. The measurements were performed using 10× magnification and 1× field of view.

2.4.2 Test Procedure

The ball-on-disk test device is used to generate friction data from a series of tests under different operating conditions. In each test, the entrainment speed and contact pressure are held constant while the slide-to-roll ratio (SRR) is varied from 0.0002 to 1.05. Both ball and disk specimens were cleaned with heptane and ethyl alcohol before starting the experiments for each of the test cases. Before starting the experiments for each test case, the test device is warmed up to the desired operating temperature during approximately 60 min with oil circulation over both ball and disk to ensure temperature stability. When stability is reached, a 80 or 300 N load, equivalent to 1.25 or 1.94 GPa maximum Hertzian pressure, is applied, and the machine is calibrated for pure rolling by adjusting spindle angle and positioning of the ball to ensure a condition of no spinning. These settings are then held constant for 20 min to ensure a mild run-in. Subsequently, the test cycle is started wherein the entrainment speed is increased from the lowest value to the largest value. The tests were repeated seven times. The temperature of the oil bulk and fluid adhered at the disk surface is typically deviating less than ±1.5 °C from the target temperature of 40 °C during testing. The actual contact temperatures are, however, higher than the bulk oil temperature. In the most severe cases with high entrainment speed, SRR and coefficient of friction (COF), the contact temperature will increase several tens of degrees.

3 Results and Discussion

The measurements conducted with coated surfaces showed significantly lower coefficients of friction compared with the uncoated reference case. The results are shown in Figs. 4, 5, 6, 7, 8, and 9. The figures show how the friction coefficient is changing with the ratio of sliding speed to rolling speed (SRR) at two different entrainment speeds. While roller bearings usually operate with low SRR, typically below 0.05, cam followers and gears operate at much higher SRR. At high sliding speeds where power losses
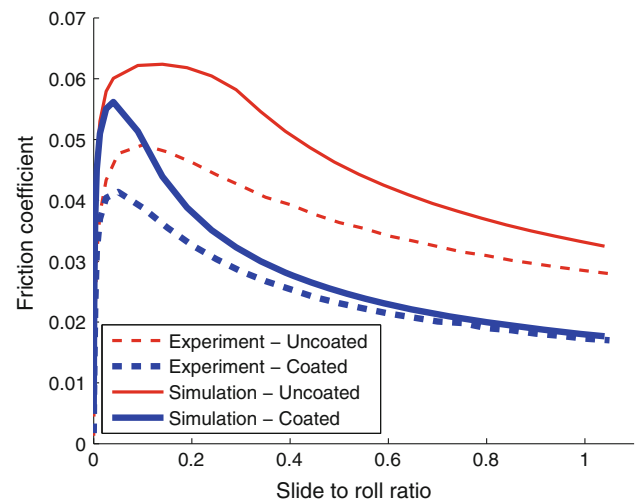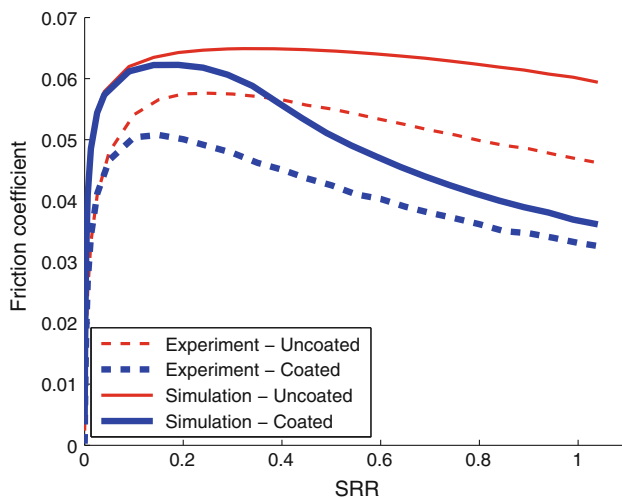

Fig. 4 Friction results at 1.25 GPa, 40 °C at 6.144 m/s entrainment speed comparing uncoated and coated specimens in both simulation and experiment
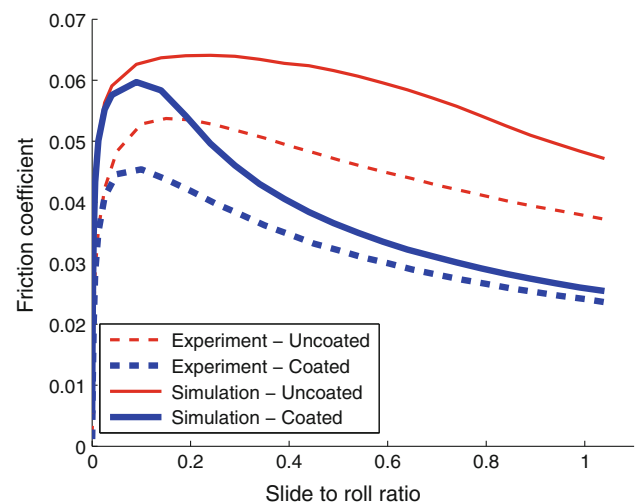
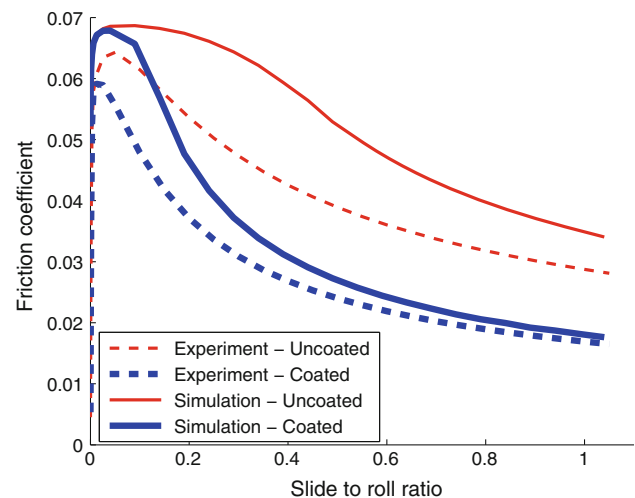

Fig. 5 Friction results at 1.25 GPa, 40 °C at 3.145 m/s entrainment speed comparing uncoated and coated specimens in both simulation and experiment

usually are the greatest, the measured reduction in friction with the coating is more than 40 % at maximum SRR for the most prominent case, Fig. 8, while at the lowest sliding speed, the decrease in friction at maximum SRR is at least 25 %, Fig. 7.

The results from the numerical simulations are shown together with the measurements in Figs. 4, 5, 6, 7, 8, and 9. Although numerically predicted friction coefficients deviate from experimental ones in absolute value, the shape and trend of the friction curves are qualitatively similar for both coated and uncoated cases. A comparison between this numerical model and some reference measurements was published recently where the discrepancy between the
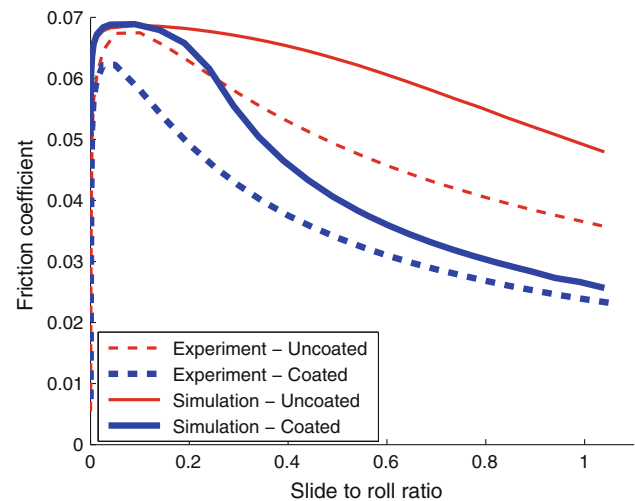
Fig. 6 Friction results at 1.25 GPa, 40 °C at 1.611 m/s entrainment speed comparing uncoated and coated specimens in both simulation and experiment

Fig. 8 Friction results at 1.94 GPa, 40 °C at 6.144 m/s entrainment speed comparing uncoated and coated specimens in both simulation and experiment
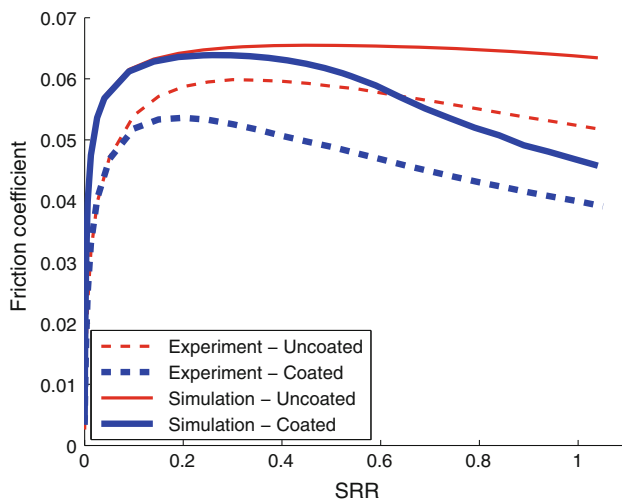

Fig. 7 Friction results at 1.25 GPa, 40 °C at 1.0 m/s entrainment speed comparing uncoated and coated specimens in both simulation and experiment

Fig. 9 Friction results at 1.94 GPa, 40 °C at 3.145 m/s entrainment speed comparing uncoated and coated specimens in both simulation and experiment

simulation results, and the measurements is discussed [5]. The simulation assumes that the solid and liquid materials are entrained into the contact at the initial bulk temperature and does not therefore account for the accumulated heat. In addition, a major part of the discrepancy might be attributed to the fact that the limiting shear stress coefficient Λ cannot be accurately deduced from traction curves as suggested by [11]. In fact, in [11] the authors show that even when the friction plateau is reached in EHL traction curves, shear-thinning in the peripheral area of the contact still affects the magnitude of friction, and therefore, the limiting shear stress coefficient cannot be directly deduced from the asymptotic friction value in the plateau region as

is the current practice in most EHL studies, including the current work. Moreover is the limiting shear stress in the numerical model used in this work assumed to be only depending on pressure. It has been shown earlier in measurements that temperature has an influence on the limiting shear stress [16]. Nevertheless, the results from the numerical predictions show that the addition of a thin (2.8 μm) thermal insulating coating leads to a substantial reduction of the friction coefficient in a lubricated EHL contact. Since the numerical model does not incorporate any chemical/surface interaction effects, such as asperity interactions or boundary slip, the observed reduction in the numerical results can only be attributed to thermal effects.
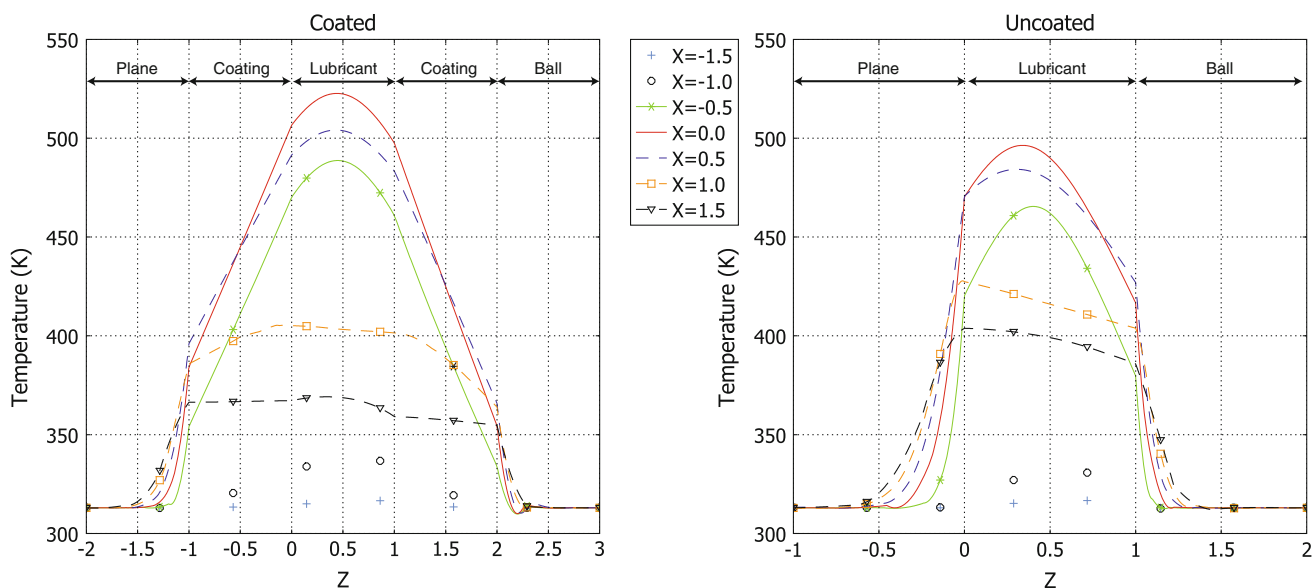
Fig. 10 Numerical simulation of lubricant film temperature increase in different locations of the lubricant film for coated and uncoated specimens
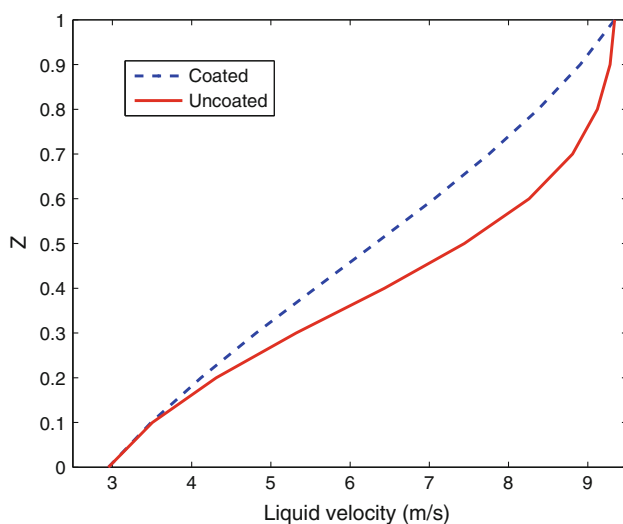
Fig. 11 Lubricant x-velocity profile at the centre of the contact across film thickness. Z = 1 is the faster moving surface (ball) and Z = 0 is the slower moving surface (disk)

Figure 10 shows the temperature distributions in the Z direction across the film and solids (substrate and coatings (for the case of coated surfaces)) from the inlet (X = −1.5) to the outlet (X = 1.5) at the same conditions as in Fig. 4. X represents the position in the circular contact in the entrainment direction. In an EHL contact the film thickness, and thus the ability to separate the surfaces from contacting each other is governed by the viscous behavior of the lubricant in the inlet of the contact. On the other hand, friction is governed by the viscous behavior of the lubricant in the central area of the contact. Therefore, a sufficiently viscous lubricant is required in the inlet to generate an adequate film thickness, while low viscosity is desirable at the contact center to reduce friction.

The difference in temperature in the inlet is very small and will thus lead to negligible differences in film thickness between the coated and uncoated case. In the central parts (X = −0.5 to X = 0.5) of the contact, there is a substantial difference in temperature in the lubricant. The higher temperature in the lubricant with the coated specimens will therefore lead to lower viscosities and consequently lower friction. However, in the outlet of the contact (X = 1.0 and X = 1.5), the lubricant temperatures are actually lower with the coating. At this stage, the lubricant film is ruptured and would therefore not contribute to the friction. The higher lubricant temperature at the contact outlet for the uncoated case results from heat transfer by conduction and advection within the solids from the center of the contact (where most of the heat is generated) toward the outlet. This leads to high solid surface temperatures at the exit of the contact, which maintains the lubricant film at a higher temperature. In the coated case, less heat is transferred to the liquid at the exit of the contact since DLC acts like an insulating material. Figure 11 shows the flow profile (the x-velocity component of the lubricant flow across the film) at the center of the contact for both coated and uncoated surfaces at the same conditions as in Fig. 4. The difference in velocity is large around the midlayer of the lubricant film and near the faster moving surface. A lower velocity variation across the lubricant film around the midlayer, and thus lower shear rates, in combination with lower viscosities due to the higher lubricant temperatures in the coated case leads to the friction reduction compared to the uncoated case.

Table 3 Friction reduction with DLC coating at SRR = 1.05

Load (N)	Entrainment speed (m/s)	Measured reduction (%)	Predicted reduction (%)
300	6.144	41	48
300	3.145	35	46
80	6.144	39	46
80	3.145	37	46
80	1.611	30	39
80	1.0	24	28

As seen in Figs. 4, 5, 6, 7, 8, and 9, the greatest reduction in friction with the coating happens at the highest SRR, as expected since more heat is generated at higher sliding speeds. Substantial friction decreases are however achieved already at much lower SRR's. Table 3 summarizes the friction reduction achieved with the coating for all entrainment speed and load cases at the highest SRR value of 1.05. It is clear that the relative reduction in friction is greatest at the highest entrainment speed and reduced when entrainment speed decrease. Note that, the relative reduction in friction is not much smaller at the low load compared with the high load. Even at the lowest load and the lowest entrainment speed, Fig. 7, the friction reduction is significant even at SRR of 0.2. This indicates that excessive heat generation is not needed to benefit from a thermally insulating coating and that SRR has greater influence on the friction reduction than contact pressure.

In this article, a coating with only one specific thermal inertia has been evaluated. The authors believes that a coating with lower thermal inertia than the one investigated will lead to greater reduction in friction, while a coating with a high thermal inertia will lead to less reduction in friction. A low thermal inertia is connected to low thermal conductivity and volumetric heat capacity and is thus insulating. It is also expected that the coating thickness will influence the friction reduction in a similar way. A thicker coating will lead to a greater friction reduction, while a thinner coating will lead to a lower friction reduction.

These findings will most likely lead to new possibilities in reducing friction in machine components working in, or partly, in the full-film EHL regime. In the experiments conducted in this study, a thermal insulating DLC coating was used, but it is certainly possible to obtain thermal insulation using other types of coatings as well. These findings will probably open the way up for new coatings (where thermal properties constitute the main design parameters) used for friction reduction in certain lubricated machine elements. These new coatings may very well be cheaper and more available than DLC coatings. The results indicate the possibility to reduce contact friction by more than 40 % using thermal insulating layers in EHL contacts.

By applying thicker coatings and/or coatings with even lower thermal conductivity even greater friction reduction could be possible.

4 Conclusions

This paper presents strong evidence that thermal insulation has an important role in friction reduction using thin coatings in full-film EHL contacts. A series of friction tests were conducted in a ball-on-disk machine with both coated and uncoated specimens. The DLC-coated specimens showed lower coefficient of friction in all tested cases. A validated TEHL numerical model was used to predict the friction coefficient for the tested cases. Although the numerically predicted values, which ignore accumulated heat, deviate from the experimental ones in absolute values, the shape and trend of the friction curves are qualitatively similar. The numerical model does not incorporate any chemical/surface interaction effects, and thus, the observed reduction in friction for the predicted results can only be attributed to thermal effects. These findings open up for the development of new families of coatings where thermal properties constitute the main design parameters. These coatings may be both cheaper to produce, more available, and provide greater friction reduction than DLC coatings in certain applications.

References

1. Bair, S.: Reference liquids for quantitative elastohydrodynamics. Tribol. Lett. **22**(2), 197–206 (2006). doi:10.1007/s11249-006-9083-y
2. Bair, S., McCabe, C., Cummings, P.T.: Calculation of viscous EHL traction for squalane using molecular simulation and rheometry. Tribol. Lett. **13**(4), 251–254 (2002). doi:10.1023/A:1021011225316
3. Bair, S., McCabe, C., Cummings, P.T.: Comparison of nonequilibrium molecular dynamics with experimental measurements in the nonlinear shear-thinning regime. Phys. Rev. Lett. **5**(4), 583021–583024 (2002). doi:10.1103/PhysRevLett.88.058302
4. Balandin, A., Shamsa, M., Liu, W., Casiraghi, C., Ferrari, A.C.: Thermal conductivity of ultrathin tetrahedral amorphous carbon films. Appl. Phys. Lett. **93**(4), 043115 (2008). doi:10.1063/1.2957041
5. Björling, M., Habchi, W., Bair, S., Larsson, R., Marklund, P.: Towards the true prediction of ehl friction. Tribol. Int. **66**, 19–26 (2013). doi:10.1016/j.triboint.2013.04.008

6. Björling, M., Isaksson, P., Marklund, P., Larsson, R.: The influence of DLC coating on EHL friction coefficient. Tribol. Lett. **47**(2), 285–294 (2012). doi:10.1007/s11249-012-9987-7

7. Björling, M., Larsson, R., Marklund, P., Kassfeldt, E.: Elastohydrodynamic lubrication friction mapping: the influence of lubricant, roughness, speed, and slide-to-roll ratio. Proc. Inst. Mech. Eng. J J. Eng. Tribol. **225**(7), 671–681 (2011). doi:10.1177/1350650111403363

8. Choo, J.H., Glovnea, R.P., Forrest, A.K., Spikes, H.A.: A low friction bearing based on liquid slip at the wall. J. Tribol. **129**(3), 611–620 (2007). doi:10.1115/1.2736704

9. Elsharkawy, A.A., Holmes, M.J.A., Evans, H.P., Snidle, R.W.: Micro-elastohydrodynamic lubrication of coated cylinders using coupled differential deflection method. Proc. Inst. Mech. Eng. J J. Eng. Tribol. **220**(1), 29–41 (2006). doi:10.1243/13506501J10005

10. Evans, R.D., Cogdell, J.D., Richter, G.A.: Traction of lubricated rolling contacts between thin-film coatings and steel. Tribol. Trans. **52**(1), 106–113 (2009). doi:10.1080/10402000802180144

11. Habchi, W., Bair, S., Vergne, P.: On friction regimes in quantitative elastohydrodynamics. Tribology I **58**, 107–117 (2013). doi:10.1016/j.triboint.2012.10.005

12. Habchi, W., Eyheramendy, D., Bair, S., Vergne, P., Morales-Espejel, G.: Thermal elastohydrodynamic lubrication of point contacts using a newtonian/generalized newtonian lubricant. Tribol. Lett. **30**(1), 41–52 (2008). doi:10.1007/s11249-008-9310-9

13. Habchi, W., Eyheramendy, D., Vergne, P., Morales-Espejel, G.: A full-system approach of the elastohydrodynamic line/point contact problem. ASME J. Tribol. **130,021501**, 1–10 (2008). doi:10.1115/1.2842246

14. Habchi, W., Eyheramendy, D., Vergne, P., Morales-Espejel, G.: Stabilized fully-coupled finite elements for elastohydrodynamic lubrication problems. Adv. Eng. Softw. **46**(1), 4–18 (2012). doi:10.1016/j.advengsoft.2010.09.010

15. Habchi, W., Vergne, P., Bair, S., Andersson, O., Eyheramendy, D., Morales-Espejel, G.E.: Influence of pressure and temperature dependence of thermal properties of a lubricant on the behaviour of circular tehd contacts. Tribol. Int. **43**(10), 1842–1850 (2010). doi:10.1016/j.triboint.2009.10.002

16. Höglund, E.: Influence of lubricant properties on elastohydrodynamic lubrication. Wear **232**(2), 176–184 (1999). doi:10.1016/S0043-1648(99)00143-X

17. Jahanmir, S., Hunsberger, A., Heshmat, H.: Load capacity and durability of h-dlc coated hydrodynamic thrust bearings. J. Tribol. **133**(3), 031,301 (2011). doi:10.1115/1.4003997

18. Kalin, M., Polajnar, M.: The correlation between the surface energy, the contact angle and the spreading parameter, and their relevance for the wetting behaviour of dlc with lubricating oils. Tribol. Int. **66**, 225–233 (2013). doi:10.1016/j.triboint.2013.05.007

19. Kalin, M., Velkavrh, I., Viintin, J.: The stribeck curve and lubrication design for non-fully wetted surfaces. Wear **267**(5–8), 1232–1240 (2009). doi:10.1016/j.wear.2008.12.072

20. Kim, J.W., Yang, H.S., Jun, Y.H., Kim, K.C.: Interfacial effect on thermal conductivity of diamond-like carbon films. J. Mech. Sci. Technol. **24**(7), 1511–1514 (2010). doi:10.1007/s12206-010-0416-2

21. Liu, Y., Chen, W.W., Zhu, D., Liu, S., Wang, Q.J.: An elastohydrodynamic lubrication model for coated surfaces in point contacts. J. Tribol. **129**(3), 509–516 (2007). doi:10.1115/1.2736433

22. Liu, Y., Wang, Q.J., Zhu, D.: Effect of stiff coatings on EHL film thickness in point contacts. J. Tribol. **130**(3), 031501 (2008). doi:10.1115/1.2908908

23. Pit, R., Hervet, H., Lger, L.: Friction and slip of a simple liquid at a solid surface. Tribol. Lett. **7**(2-3), 147–152 (1999). doi:10.1023/A:1019161101812

24. Pit, R., Hervet, H., Lger, L.: Direct experimental evidence of slip in hexadecane: solid interfaces. Phys. Rev. Lett. **85**(5), 980–983 (2000). doi:10.1103/PhysRevLett.85.980

25. Reynolds, O.: On the theory of lubrication and its application to mr beuchamp tower's experiments, including an experimental determination of the viscosity of olive oil. Philos. Trans. R Soc. **177**, 157–234 (1886)

26. Shamsa, M., Liu, W., Balandin, A., Casiraghi, C., Milne, W., Ferrari, A.: Thermal conductivity of diamond-like carbon films. Appl. Phys. Lett. **89**(16), 161921 (2006). doi:10.1063/1.2362601

27. Spikes, H.A.: The half-wetted bearing. Part 1: Extended reynolds equation. Proc. Inst. Mech. Eng. J J. Eng. Tribol. **217**(1), 1–14 (2003). doi:10.1243/135065003321164758

28. Spikes, H.A.: The half-wetted bearing. part 2: Potential application in low load contacts. Proc. Inst. Mech. Eng. J J. Eng. Tribol. **217**(1), 1–14 (2003). doi:10.1243/135065003321164776

29. Thompson, P., Troian, S.: A general boundary condition for liquid flow at solid surfaces. Nature **389**(6649), 360–362 (1997). doi:10.1038/38686

30. Tower, B.: Second report on friction experiments (experiments on the oil pressure in a bearing). Proc. Inst. Mech. Eng. pp. 58–70 (1885)

31. Wong, P., Li, X., Guo, F.: Evidence of lubricant slip on steel surface in ehl contact. Tribol. Int. **61**, 116–119 (2013). doi:10.1016/j.triboint.2012.12.009

32. Xu H. (2005) Development of a generalized mechanical efficiency prediction methodology for gear pairs. Ph.D. thesis, Graduate School of The Ohio State University

33. Yang, P., Wen, S.: A generalized reynolds equation for non-newtonian thermal elastohydrodynamic lubrication. J. Tribol. **112**(4), 631–636 (1990)

34. Zhu, Y., Granick, S.: Rate-dependent slip of newtonian liquid at smooth surfaces. Phys. Rev. Lett. **87**(9), 961051–961054 (2001). doi:10.1103/PhysRevLett.87.096105

35. Zhu, Y., Granick, S.: Limits of hydrodynamic no-slip boundary condition. Phys. Rev. Lett. **88**(10), 1061021–1061024 (2002). doi:10.1103/PhysRevLett.88.106102